Fine tuning plasmonic properties of monolayers of weakly interacting silver nanocubes on thin silicon films

Adam Bottomley, Daniel Prezgot, Alyssa Staff, Anatoli Ianoul

Department of Chemistry, Carleton University, 1125 Colonel By Dr. Ottawa ON Canada

Phone: (613)-520-2600 x 6043, Fax: (613)-520-3749

KEYWORDS: Silver nanocube monolayer, silicon film, plasmon mode hybridization, refractive index sensing, SERS, fluorescence quenching, photodegradation.

Table S1: Refractive index sensitivities of monolayers of 35-40 nm silver nanocubes on silicon

Silicon film thickness/ nm	Plasmon peak position λ/nm	Refractive index sensitivity (nm/RIU)	Figure of merit
5	D: 417	77+/-5.4	1.38
	Q: 382	28+/-8	0.74
	350	44+/-5.3	2.4
10	D: 427	42+/-8.1	0.72
	Q: 388	**70+/-23**	**2.22**
	350	n.d.[a]	n.d.
25	D: 440	11+/-8	0.18
	Q: 395	**76+/-6**	**2.0**
	350	48+/-0.5	1.12

[a] Not determined.

Table S2: Refractive index sensitivities of monolayers of 40-45 nm silver nanocubes on silicon

Silicon film thickness/ nm	Plasmon peak position λ/nm	Refractive index sensitivity (nm/RIU)	Figure of merit
5	D: 427	82+/-3.4	1.45
	Q: n.d.[a]		
	350	25+/-0.57	1.64
10	D: 440	25+/-12	0.76
	Q: 407	**95+/-4**	**3.73**
	350	28+/-1.1	1.82
25	D: 460	48+/-4.6	0.93
	Q: 408	**96+/-6.8**	**2.67**
	350	27+/-3.4	1.60

[a] Not determined.

Table S3: Refractive index sensitivities of monolayers of 75-80 nm silver nanocubes on silicon

Silicon film thickness/ nm	Plasmon peak position λ/nm	Refractive index sensitivity (nm/RIU)	Figure of merit
0	D: 483	330+/-104	1.34
	Q: 445	114+/-15	**1.57**
	360	65+/-13	1.34
	340	26+/-2.7	1.46
15	D: 500	120+/-43	0.6
	Q: 452	**125+/-50**	**2.3**
	360	76+/-9.7	1.32
	340	28+/-5.7	1.2
25	D: 600	8.2+/-5.6	0.1
	Q: 455	**140+/-37**	**1.44**
	385	74+/-25	1.23
	350	13+/-3	0.41

Table S4: Refractive index sensitivities of monolayers of 80-85 nm silver nanocubes on silicon.

Silicon film thickness/ nm	**Plasmon peak position λ/nm**	**Refractive index sensitivity (nm/RIU)**	**Figure of merit**
0	D: 487	480+/-88	3.0
	Q: 445	174+/-6	2.4
	382	94+/-42	**4.4**
	350	18+/-7.8	1.1
10	D: 494	64+/-1	0.38
	Q: 446	**237+/-17**	**6.6**
	385	113+/-7.4	3.0
	350	58+/-1.7	3.1
15	D: 504	49+/-9	0.28
	Q: 445	**174+/-10**	**3.3**
	383	93+/-7	2.65
	350	57+/-9	3.2
16	D: 502	35+/-22	0.6
	Q: 443	**124+/-6**	**3.46**
	383	69+/-5	2.0
	350	39+/-1	2.6
25	D: 547	45+/-9	0.1
	Q: 450	**167+/-4.6**	2.35
	383	148+/-8.4	**4.0**
	350	61+/-5.7	3.21

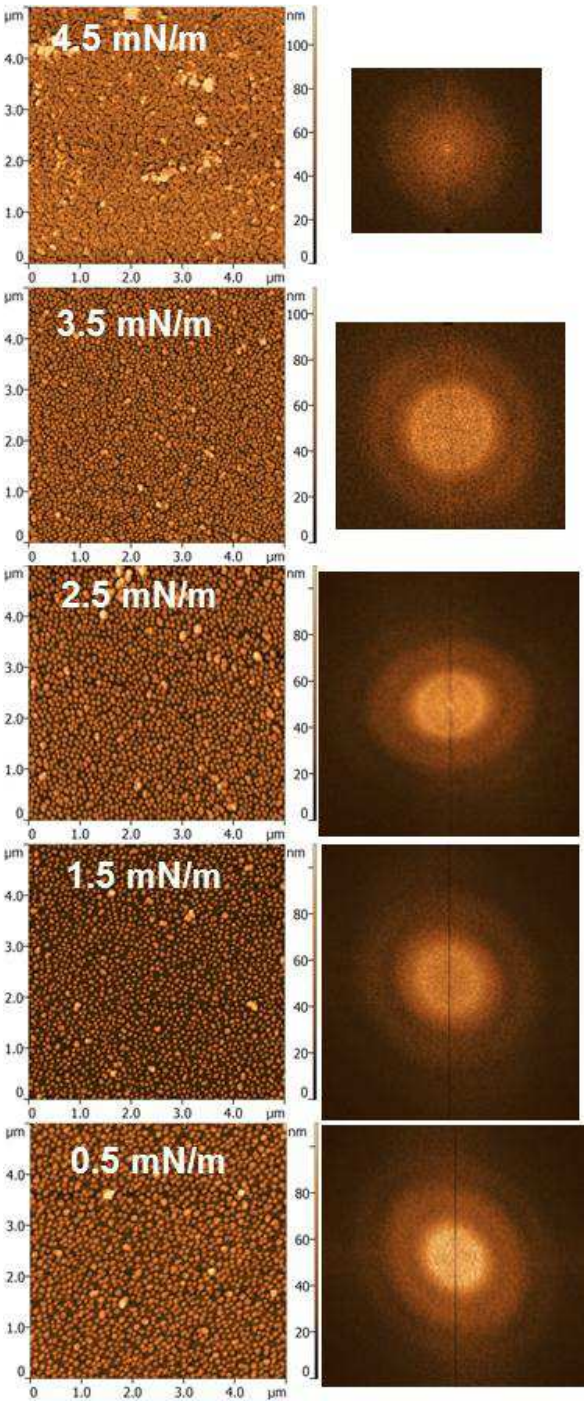

Figure S1. Left column: AFM topography images of monolayers of 35-40 nm silver nanocubes/ DOPC deposited on a 15 nm thick silicon film at various surface pressures, as indicated. Right column: corresponding Fast Fourier transformation images corresponding to the images on the left side. Concentric circles indicate the presence of short range order (middle to middle, the smallest circle), and the particle size (second circle) respectively. The third concentric circle indicates the separation between the particles (side to side). Short range order disappears at high surface pressure of 4.5 mN/m.

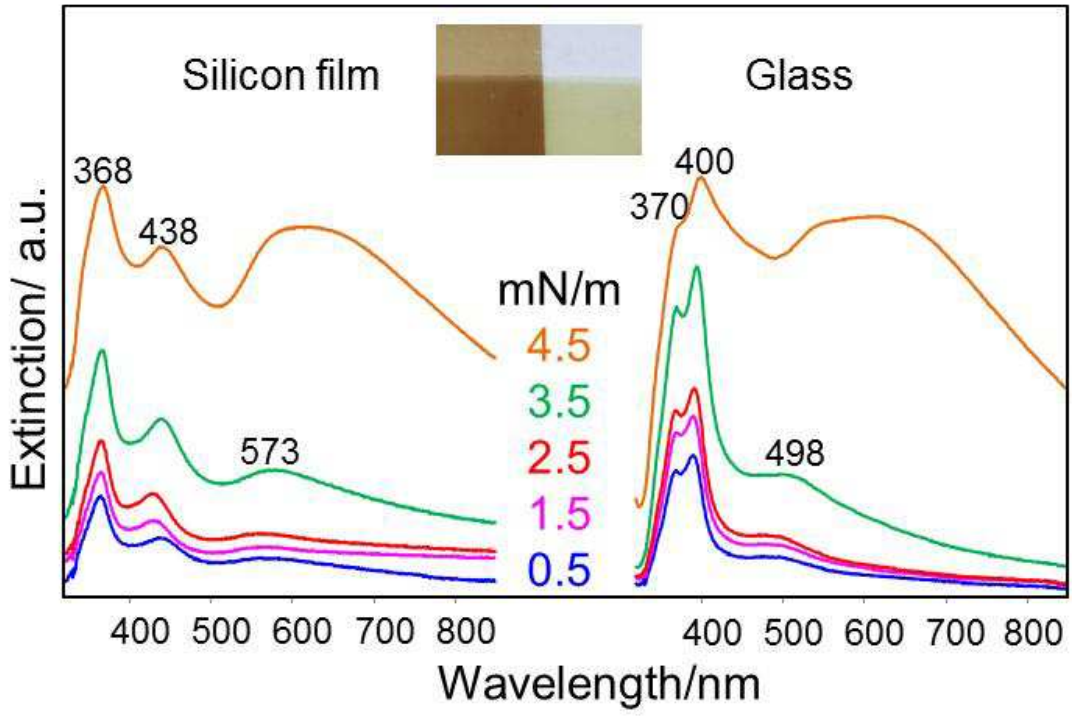

Figure S2: UV-vis extinction spectra for monolayers of 35-40 nm silver nanocube/ DOPC deposited at various surface pressures on a 15 nm silicon film (left) or glass slide (corresponding to figure S1 images). Deposition was performed simultaneously onto glass and silicon sides of the substrate. The strong dipole-dipole coupling peak becomes dominant at high surface pressure of 4.5 mN/m. The photo shows s slide with silicon film on the left hand side. The bottom part of the slide is coated with the nanocube/DOPC monolayer.

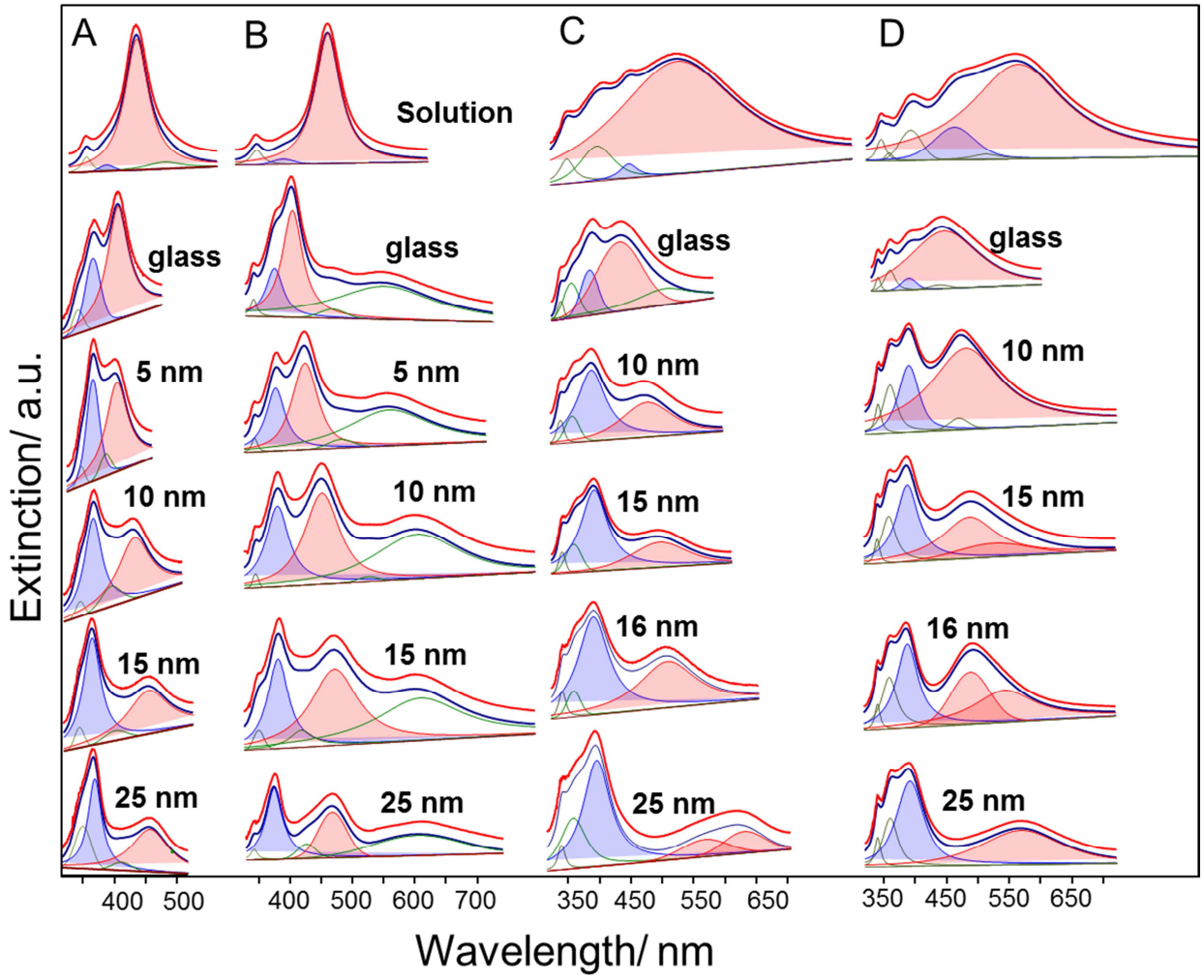

Figure S3: Results of extinction spectra deconvolution for silver nanocubes in ethanol solution (the top most spectra) and for nanocube/ DOPC monolayers deposited on different substrates in air. Series in columns correspond to samples A, B, C, and D (from left to right) in Figure 2. Red thick curves represent experimental data. Dark blue thick curves represent results of spectral fitting. Blue and red peaks correspond to quadrupolar and dipolar modes respectively. Silicon film thickness is indicated.

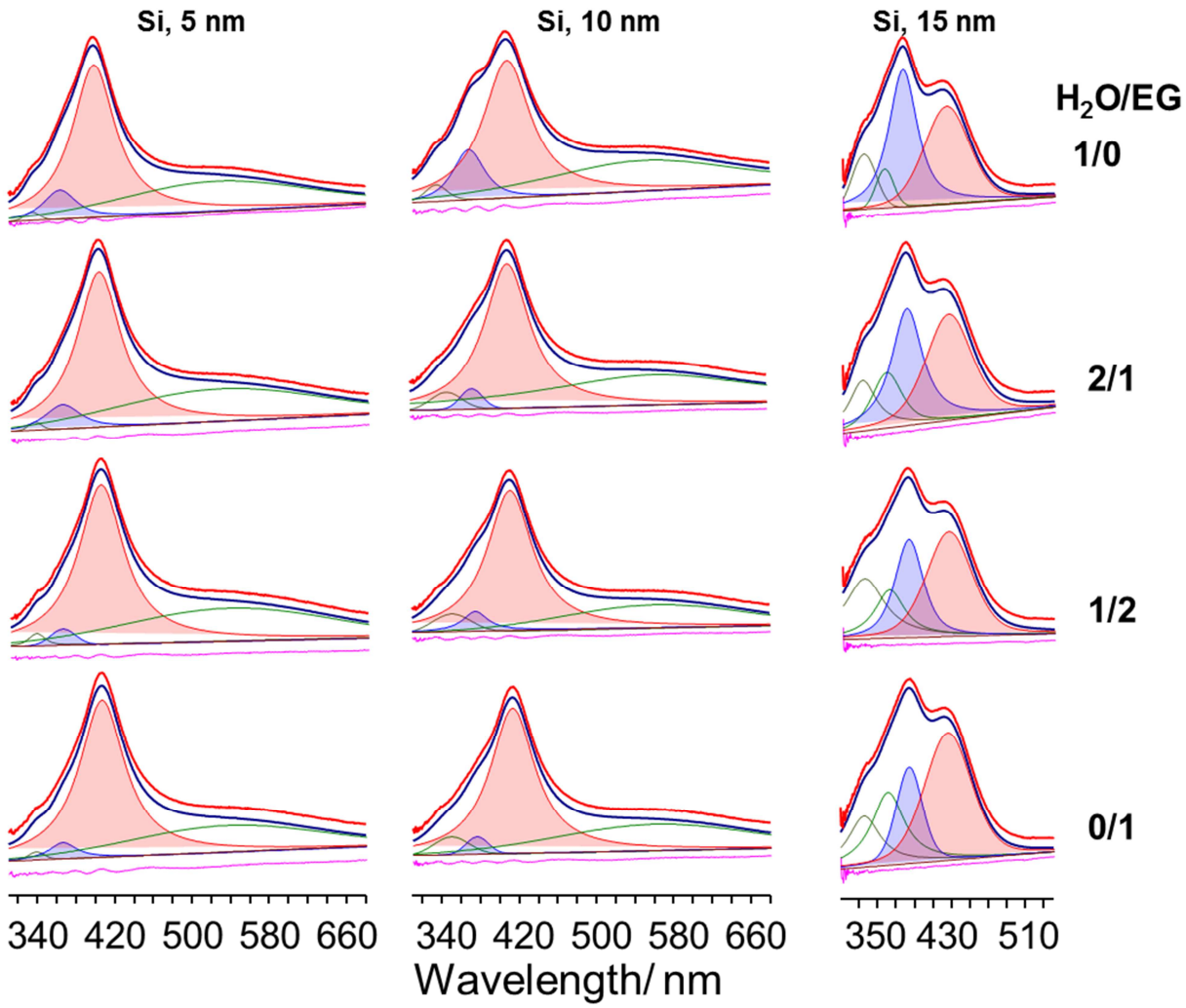

Figure S4: Results of extinction spectra deconvolution for 35-40 nm silver nanocubes/ DOPC monolayers deposited on different silicon films immersed in water/ethylene glycol mixtures 1/0, 2/1, 1/2, and 0/1 volume ratios. Series correspond to the sample A in Figure 5. Red thick curves represent experimental data. Dark blue thick curves are the result of spectral fitting. Purple lines show the difference between the fitted and experimental spectra. Blue and red peaks are quadrupolar and dipolar modes respectively.

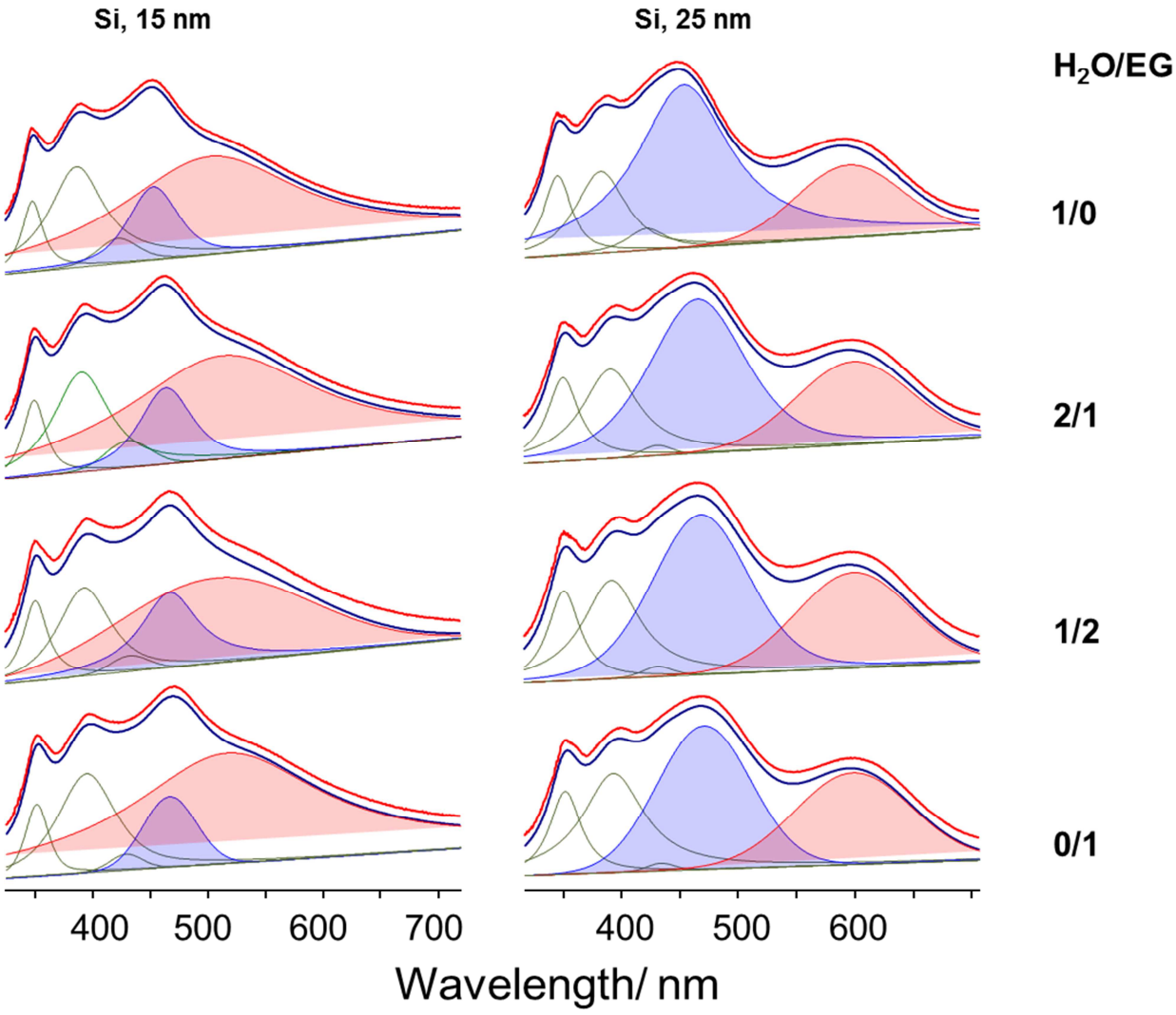

Figure S5: Results of extinction spectra deconvolution for 75-80 nm silver nanocubes/ DOPC monolayers deposited on different silicon films immersed in water/ethylene glycol 1/0, 2/1, 1/2, and 0/1 volume ratios. Series correspond to the sample C in Figure 5. Red thick curves represent experimental data. Dark blue thick curves are the result of spectral fitting. Blue and red peaks are quadrupolar and dipolar modes respectively.

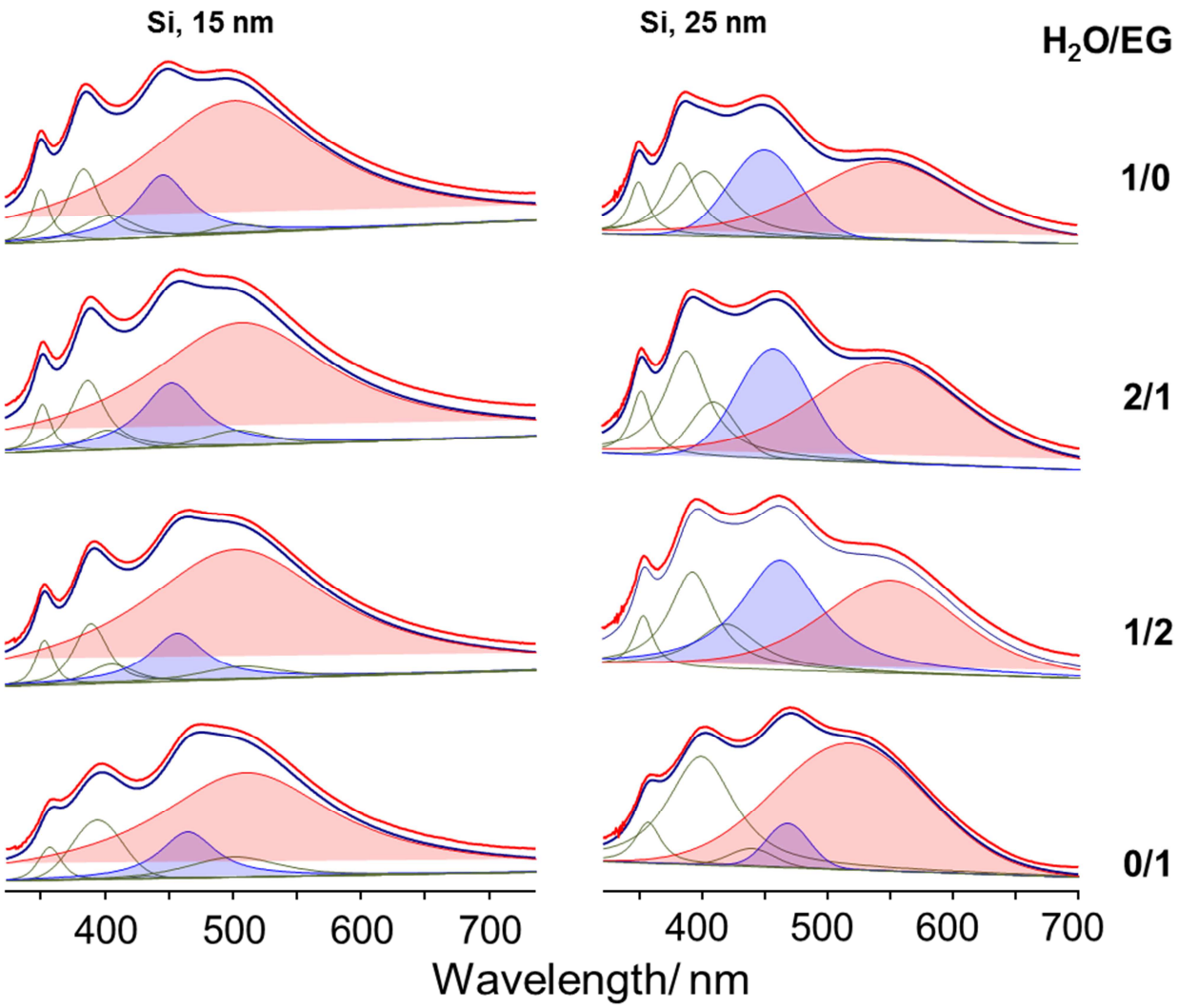

Figure S6: Results of extinction spectra deconvolution for 80-85 nm silver nanocubes/ DOPC monolayers deposited on different silicon films immersed in water/ethylene glycol 1/0, 2/1, 1/2, and 0/1 volume ratios. Series correspond to sample D in Figure 5. Red thick curves represent experimental data. Dark blue thick curves are the result of spectral fitting. Blue and red peaks are quadrupolar and dipolar modes respectively.

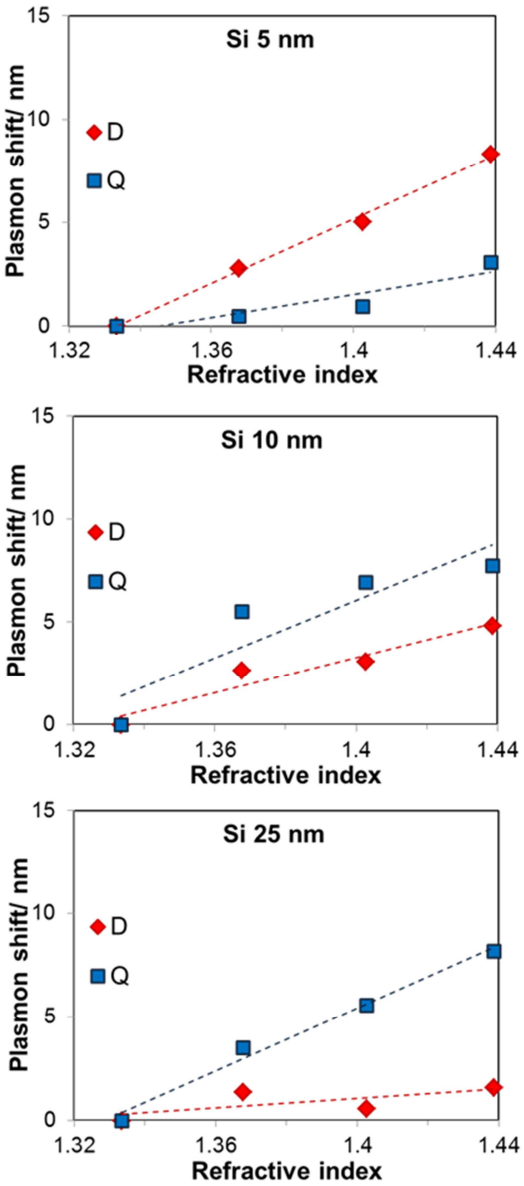

Figure S7A: Plasmonic shifts as functions of solution refractive index for supported nanocube/ DOPC monolayers in figure 5A.

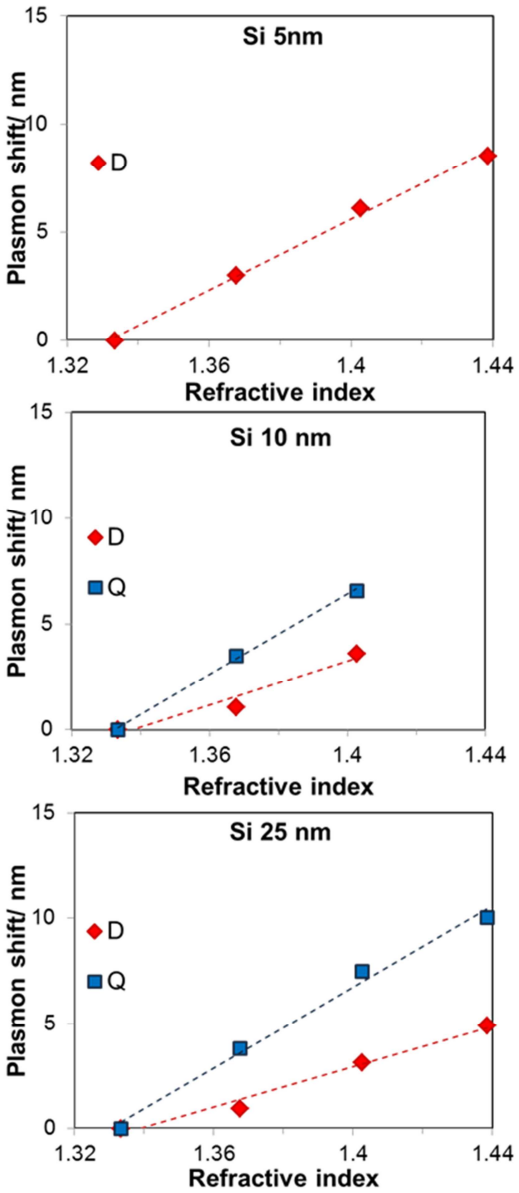

Figure S7B: Plasmonic shifts as functions of solution refractive index for supported nanocube/ DOPC monolayers in figure 5B.

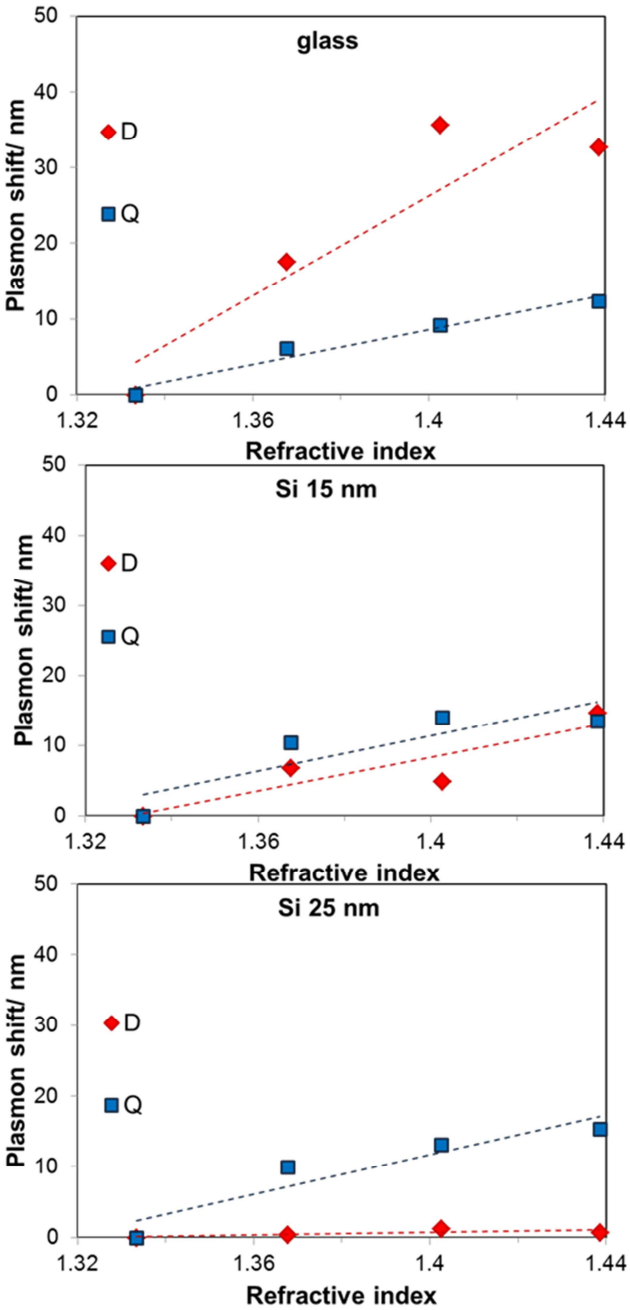

Figure S7C: Plasmonic shifts as functions of solution refractive index for supported nanocube/ DOPC monolayers in figure 5C.

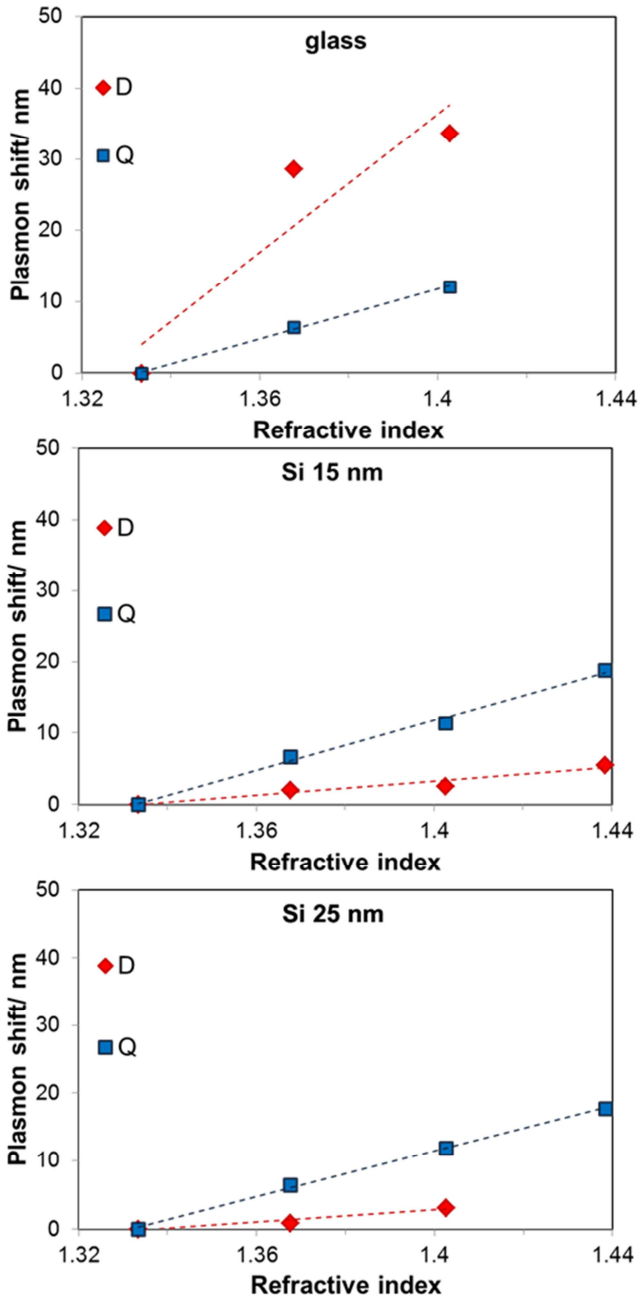

Figure S7D: Plasmonic shifts as functions of solution refractive index for supported nanocube/ DOPC monolayers in figure 5D.

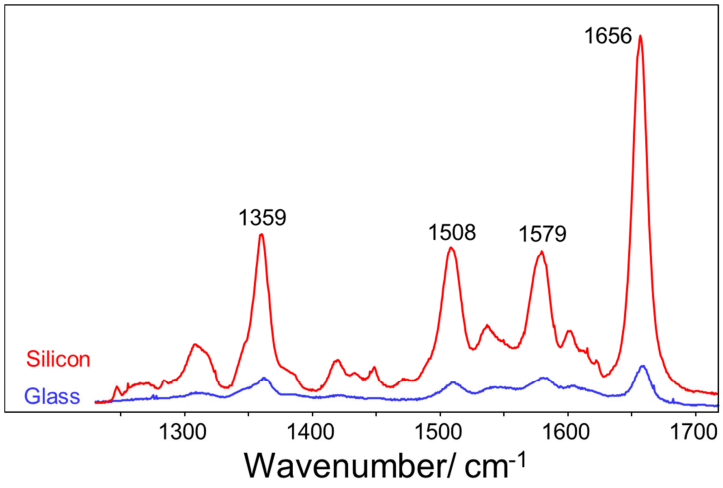

Figure S8. SERS spectra of Rhodamine 6G (1 μM) deposited on a monolayer of ~60 nm silver nanocubes/DOPC on glass (blue) and 7 nm silicon film (red). The spectra were obtained by averaging spectra from 9 different areas of the sample. Accumulation time in each point was 60 seconds. Excitation wavelength used was 458 nm with laser power below 1 mW.

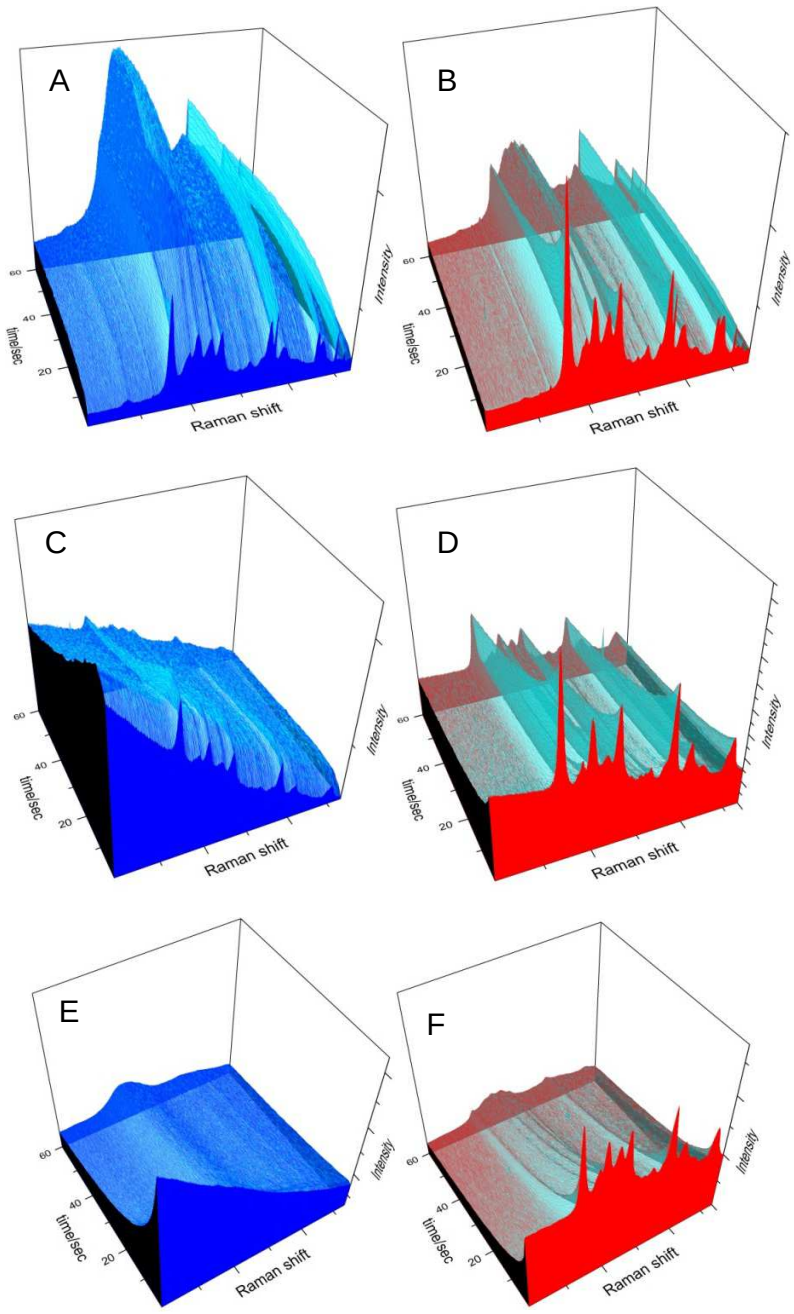

Figure S9. SERS spectra of Rhodamine 6G (1 μM) deposited on a monolayer of ~60 nm silver nanocubes/DOPC on a glass (A,C,E, blue surfaces) and 7 nm silicon film (B,D,F, red surfaces). Time progression of the spectra over 60 seconds is presented. Excitation wavelength of 458 (A,B) or 488 (C-F) nm was used. Laser power was 25 mW (A,B); 5 mW (C,D), and 50 mW (E,F).